Ion Thruster Performance Calibration

EUGENE V. PAWLIK,* RAYMOND GOLDSTEIN,† DENNIS J. FITZGERALD,‡ AND ROY W. ADAMS§
Jet Propulsion Laboratory, Pasadena, Calif.

The calibration of a typical 20-cm-diam ion thruster was examined to determine performance penalties that must be assessed in projecting measured performance into a space environment. Four specific areas were investigated. These include sources of error inherent in the thruster (double ion content of the beam and beam spreading); and error sources peculiar to the test facility (back ingestion from the vacuum chamber and propellant flow rate measurements). The double ion content was measured and found to be as high as 5.5% at an arc voltage of 35 v. Beam spreading reduced effective thrust on the order of 2.5%. Back ingestion was observed to become significant above tank pressures of 6×10^{-6} torr.

Introduction

NUMEROUS mission studies in recent years have examined the possibility of using electron-bombardment mercury ion thrusters in a solar electric spacecraft for deep-space missions.[1-5] To give an accurate picture of the capabilities of such spacecraft, the detailed mission analysis must include an accurate evaluation of thrust subsystem efficiencies and limitations. The purpose of the present study was to identify and establish the extent of thrust uncertainty in present thrust subsystem performance predictions.

Thrust uncertainties in a propulsion subsystem can, in general, be cataloged into two separate groupings, identified perhaps as a priori and in-flight dispersons. The a priori category includes performance uncertainties that would fall into two areas, calibration and time dependent variations. Performance calibration includes items not customarily taken into account in thruster performance figures. This calibration would assess penalties due to double ion content and ion beam spreading. In addition, errors introduced by effects of the laboratory test procedure must be identified and assessed. Included here are interactions between the thruster and the finite pressure in the test chamber, and inaccuracies in propellant flow rate measurement. These are characteristic of each individual test facility, but must nevertheless be evaluated. Time dependent variations would incorporate predictable effects on system performance, expected as a result of power matching or the erosion and deterioration of various thruster elements such as the cathode, neutralizer, and accelerator grid.

In-flight dispersions would include effects on system performance that result from unpredictable variations in the regulation of various power supplies, drifts in reference voltages for the power conditioner control loops, variations in the thruster magnetic field as a result of operating temperatures, or aging of components. The number of system recycles that might be required in order to clear shorts or protect the power conditioning units and their effect on the spacecraft would also fall into this category.

The present study has attempted to detail one facet of the general problem of thrust subsystem dispersions described above. The calibration of a typical 20-cm-diam ion thruster was examined to 1) determine the performance penalties that must be assessed in projecting measured performance into the space environment and 2) develop techniques that adequately assess these penalties.

Presented as Paper 72-475 at the AIAA 9th Electric Propulsion Conference, Bethesda, Md., April 17-19, 1972; submitted April 26, 1972; revision received December 26, 1972. This work presents the results of one phase of research carried out in the Propulsion Research and Advanced Concepts Section of the Jet Propulsion Laboratory, California Institute of Technology, under Contract NAS7-100, sponsored by NASA.

Index category: Electric and Advanced Space Propulsion.

*Acting Group Supervisor. Member AIAA.
†Member Technical Staff.
‡Engineer. Student Member AIAA.
§Engineering Assistant. Member AIAA.

Apparatus

Tests were performed with a 20-cm-diam electron bombardment ion thruster operated in a 0.914-m-diam by 2.13-m-long vacuum chamber. The basic elements of this type of thruster along with power supplies and control loops are shown in Fig. 1. The nominal operating level for this thruster is 1000–2000 w (0.5–1.0 amp of ion beam current at a net acceleration voltage of 2000 v) of throttleable output beam power. Accelerator voltage, unless otherwise noted, was maintained at -1000 v. The details of thruster construction and performance can be found in Refs. 6 and 7. Mercury propellant was supplied to the discharge chamber and hollow cathode by two electrically heated porous tungsten vaporizers. The liquid mercury was supplied to each vaporizer from its own precision bore glass tube reservoir. A plasma bridge neutralizer was located about 1.5 m downstream of the thruster and was operated during all testing.

Two instruments were developed to investigate the ion beam. These were 1) a mass spectrometer and 2) a collimated current density probe. Their construction and installation are described below. Each instrument was set up and aligned optically before each test and checked afterward.

Mass Spectrometer

A simple mass spectrometer utilizing a variable magnetic field was used to separate different charge to mass ratio ions in a small sampling of the total thruster exhaust beam. Design details are given in Ref. 8.

The location of the mass spectrometer in relation to the ion thruster is shown in Fig. 2. Rotational movement of both the thruster and spectrometer were provided and measured by a voltage applied to a 10-turn potentiometer. These were intended initially to obtain maximum signal from the instrument. These movements proved useful in observing variations in ion content across the thruster diameter.

Current Density Probe

A probe was also constructed to measure the beam from a small circular portion of the thruster in a manner somewhat similar to the one described in Ref. 9. Details of this probe are presented in Fig. 3. The unit consisted of 1) three collimation apertures, 2) a bias cylinder, and 3) a collector. The three collimating apertures contained 0.25-cm-diam holes which

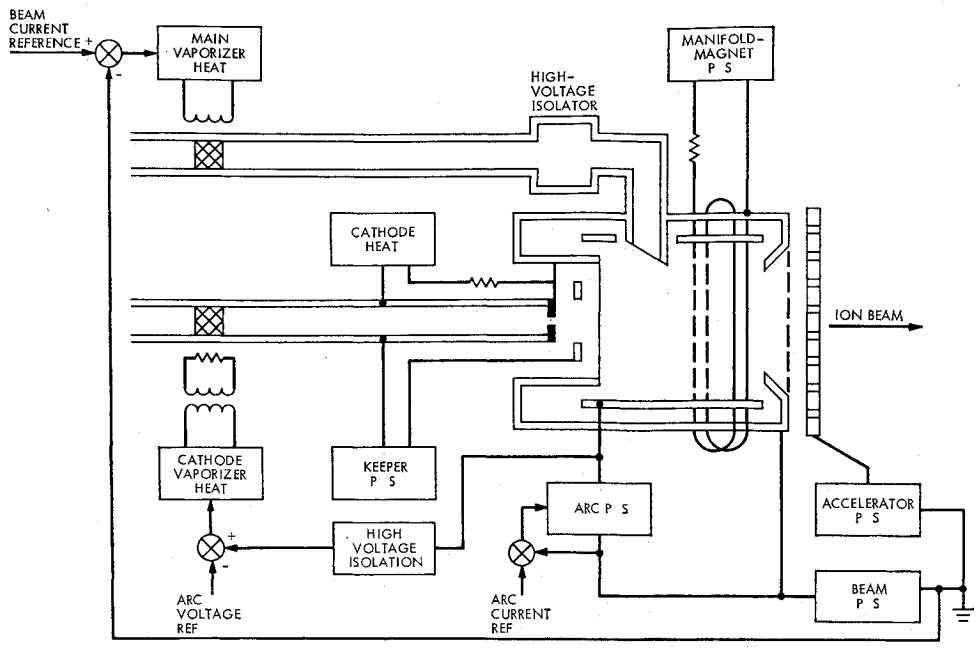

Fig. 1 Ion thruster schematic.

permitted viewing of a 2.0-cm-diam portion of the accelerator grid surface from a distance of 61 cm. The size of the area viewed was chosen so as to minimize variations in open to total area ratio along the grid surface as the probe traversed the grid diameter. A bias surface was used to suppress electrons entering or leaving the collector. The collector geometry was arranged so that a minimum of sputtered material or secondary electrons was able to leave directly.

The location of the current density probe in relation to the thruster is shown in Fig. 4. Rotation of the thruster and a linear translation of the probe were provided by servomotors and measured by a voltage applied to a 10-turn potentiometer. The probe was allowed to traverse a radial line on the grid surface. The thruster rotated about this same radial line, thus providing a direct indication of the beam spreading along a radial line. The collector current was amplified and plotted against radial position of the probe.

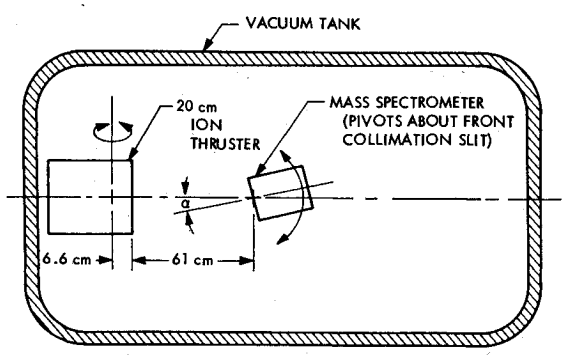

Fig. 2 Thruster and spectrometer position in vacuum facility.

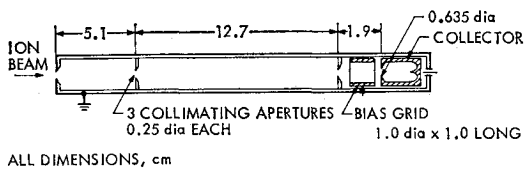

Fig. 3 Schematic diagram of collimated current density probe.

Results and Discussion

The spreading of the ion beam, double ion content of the beam, back ingestion from the vacuum tank into the thruster, and determination of the mercury propellant flow rate were examined in detail. Each of these areas will be discussed in turn.

Ion Beam Spreading

Initial attempts to determine the beam spreading utilized planar current density probes of the type used in Refs. 10 and 11. Although this approach can locate the center of the beam, it proved inadequate for determining beam spreading since current arriving at this probe came from many portions of the thruster and indicated different average angles of beam spreading as the distance between the thruster and plane of the probes was varied. A test setup using a highly collimated current density probe was therefore selected. The technique used here extends the method first presented in Ref. 9. It varies from the prior approach inasmuch as only a small area of the thruster face is examined by the probe and, more importantly, the thruster surface is traversed in such a manner as to provide a direct indication of the beam spreading and allow the axial component of the thrust to be calculated with a minimum of complexity.

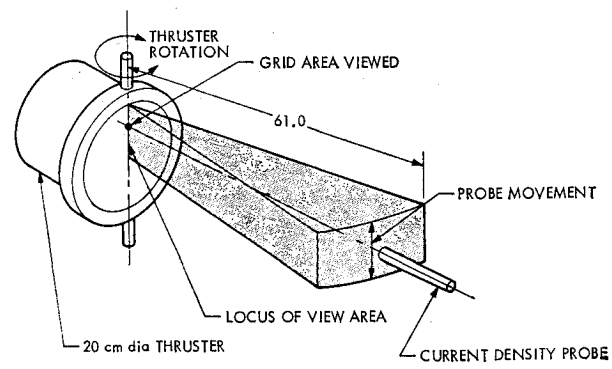

Fig. 4 Experimental setup for determining beam spreading.

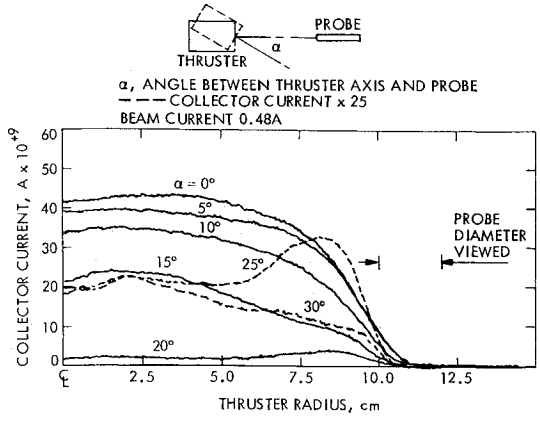

Fig. 5 Collimated current density probe traces.

Beam spreading was determined assuming that the ion beam was symmetric around the normal axis to the accelerating grid at each radial location on the grid surface. A radial line on the accelerator grid surface was traversed as the current to the collector of the current density probe was recorded. Typical results are shown in Fig. 5 for several settings of the angle between the thruster and the probe. These traces were obtained for a beam current of 0.48 amp. Similar data were obtained for other levels of beam current. In each case the thruster was rotated by a servomotor and gear train to provide incremental variations in the angle between the probe and thruster up to a maximum of 31°. All probe current traces went to zero as the center of the area under focus by the probe moved beyond the working area of the accelerator grid by 1.0 cm (radius of the area being viewed). No current was collected as the probe focussed entirely on regions of the beam outside of this area. Each trace verified the same location of the edge of the ion extracting region of the accelerating grid. The traces obtained at wide angles of view (25° or greater) were very small and therefore were plotted at increased amplification. This permitted more accurate determination of the current density in this region. The noise to signal ratio was observed to be quite small even at increased amplification and no shift in the zero level was found with the increased gain of the current measuring instruments. A greater beam spreading at the periphery of the beam diameter than nearer the center was easily discernible with this measuring technique. This increased spreading was verified by a visual observation of the accelerator grid. After several thousand hours of operation, evidence of direct impingement was noticeable at the outer holes.

Two cross plots of the data of Fig. 5 are shown in Fig. 6. Using this type of plot and the calculation procedure outlined

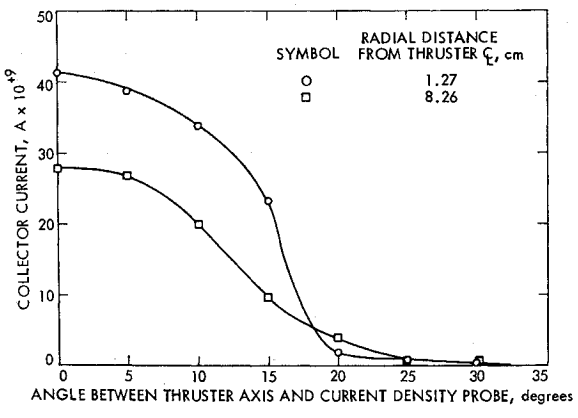

Fig. 6 Off axis current density distribution.

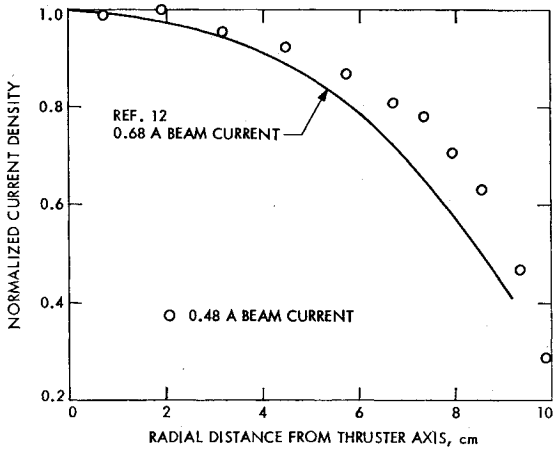

Fig. 7 Thruster current density distribution, beam current, 0.48 amp

in Ref. 8, the relative current density and the thrust efficiency (ratio of the axial component to total current density) at several locations on the accelerator grid was determined. Normalized current density along a thruster radius is presented in Fig. 7 for the 0.48 amp beam current condition. The ion density profile measurements inside a similar thruster given in Ref. 12 is also shown in the figure for comparison. Reasonable agreement between the two methods of determining the ion density at the grid surface was demonstrated.

The total loss in axial thrust at each operating point was determined by integrating the product of ion density and thrust efficiency across the grid surface and dividing this integral by the beam current. The results of these calculations are plotted in Fig. 8 for several levels of beam current. This loss decreased slightly with beam current. A nominal thrust loss of 2.5% was found to exist for the thruster examined These results are consistent with those presented in Ref. 9.

Double Ion Content

Operation of one of the first versions of an electron bombardment thruster with a mass spectrometer was reported in the early exploratory results of Ref. 13. This experiment provided good order-of-magnitude measurements and the need to account in thruster performance for double ion content. However, limits on data reliability existed mainly as a result of the extremely low resolution of the spectrometer. Thruster instability at some operating conditions also limited the range of available data. The need for more accurate and definitive data on present thruster designs for detailed mission performance analysis led to the development of the higher resolution instrument used in this investigation.

The width of the resolution slit was investigated to determine whether the entire beam passing through the instrument arrived at the collector. The results were found to be unaffected for slit widths greater than 0.12 cm. The slit width of 0.38 cm used in obtaining the results was wider than required giving some overlap between the single and double ion peaks.

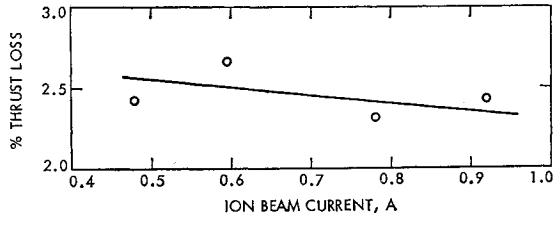

Fig. 8 Effect of beam current on thrust loss due to beam spreading; net accelerating voltage 2000 v, total voltage 3000 v.

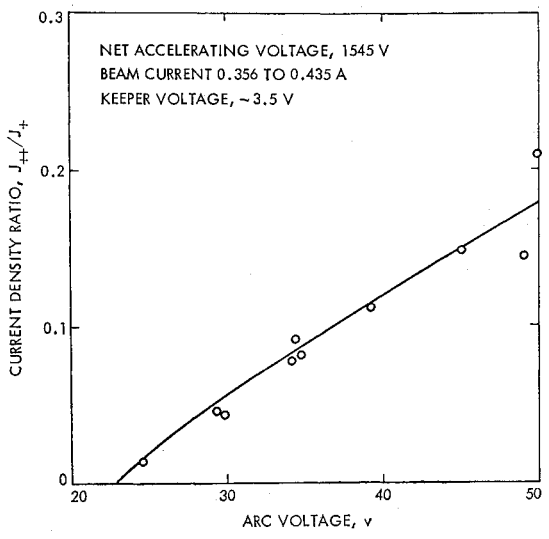

Fig. 9 Effect of arc voltage on double ion content.

The contribution of the single ion species was subtracted from the double ion peak and the double to single ionized mercury current density fraction was taken to be the ratio of this difference to the single ion peak.

In obtaining these data, the thruster and spectrometer were both rotated until maximum signals were obtained. Figure 9 gives the double to single ion current ratio at a location near the thruster centerline for a range of discharge voltage. This fraction was found to vary with the arc discharge potential in the manner previously described in Ref. 13. The results were of the same magnitude as those presented in Ref. 14. The 23-v level at which the double ion species could be detected suggests that ionization is occurring from other than the neutral ground state. Data scatter near 50 v was felt to be a result of unstable thruster operation where a long settling time for the thruster to reach equilibrium conditions was not obtainable after a change in discharge voltage. A surprising variation in double to single ion current density ratio as the thruster diameter was traversed was observed and is presented in Fig. 10. Several levels of current to the thruster electromagnets were examined and found not to affect the variation of the ratio to any significant degree. The ratio was found to vary about 2.5:1 over the thruster diameter. An average value was therefore required in order to determine thruster losses. Using the data of Fig. 10 along with the current density distribution of Fig. 7 an average ratio of 0.064 was calculated. The net accelerating voltage for the data was 1535 v. The effect of net accelerating voltage on the data was found to be small, however. The average ratio corresponds to 3.2% of the beam current being comprised of doubly ionized mercury atoms. The presence of double ions results in a loss in effective thrust of almost 2% compared to a beam with no double ions. The double ions also increase the

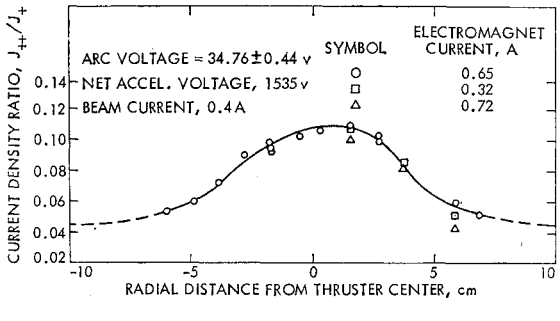

Fig. 10 Variation in double ion content across thruster diameter.

average beam exhaust velocity 1.3% and reduce the apparent propellant utilization 3.2%. At an apparent propellant utilization of 90% the effective specific impulse is reduced 1.9% by the double ion content.

The observed variation of double ion fraction with position was of interest. The change in the ratio of these species across the beam can be understood by considering details of ion production as a function of position within the discharge chamber. The following ionization processes are important for single ion production: 1) by primary electrons from the atomic ground state, 2) by thermal electrons from the atomic ground state, 3) by primary electrons from an atomic excited state, and 4) by thermal electrons from an atomic excited state. Processes 3 and 4 have previously been neglected in analyses of ionization in mercury thrusters. However, their contribution is comparable to that of 1 and 2. Double ionized mercury is produced by the following: 5) by primary electrons from the atomic ground state, 6) by thermal electrons from the atomic ground state, 7) by primary electrons from the single ion ground state, and 8) by thermal electrons from the single ion ground state. Again, although the two-step processes 7 and 8 have previously been neglected their contribution can be comparable to that of the one-step processes.

Numerical calculations have been carried out to estimate the production rate due to the above eight processes. Magnetic fields were ignored in making these calculations. For 3 and 4 the 5.7 ev metastable level was used as the intermediate state. Values of densities were taken from the measurements of Masek.[12] Published experimental cross sections were used for 1 and 5 (Ref. 15). For simplicity classical Gryzinski cross sections were used for 2, 4, 6, and 8 (Ref. 16). Scaled experimental values were used for 3 and 7. Although this procedure is only approximate, it is a simple and consistent method of analyzing the problem. Strictly speaking, these rates should be integrated over the entire discharge chamber. However, since the calculation is already only approximate it was felt that it would suffice to examine the rates only near the screen grid. Sample calculations show that contributions from other parts of the thruster are probably not significant.

The results of the calculations predict that the ratio of on-axis to off-axis double ion fraction due to variations in the plasma density should be about 2.5. This is in good agreement with the observed variation described above (Fig. 10). It should be pointed out that if the two-step ionization processes are neglected, the calculations predict a higher double ion fraction near the beam edge. This is clearly not the case.

Back Ingestion

Operation of an ion thruster in a finite size test facility with a finite speed pumping system results in a small backflow or "ingestion" of background atoms and molecules through the accelerator grids into the discharge chamber. This background consists of residual air molecules, vacuum pump oil, material sputtered and outgassed from the vacuum chamber walls, and mercury. The amount of this ingestion depends on details of the test facility and results in an increase in measured beam current.

In order to determine accurately the true thruster performance from the measured test data, some estimate must be made of the effects of this ingestion. In order to assess these effects, experimental and analytical studies were made with the thruster operating in the test facility. Figure 11 shows the experimental arrangement. A controlled N_2 leak was allowed to increase the chamber pressure over its normal operating value, while engine performance characteristics were determined. Chamber pressure was measured in two locations, one (nude) ionization gage was located at the chamber end-bell near the thruster while the other was located in the elbow connecting the chamber to the pumping system. Although, as mentioned previously, the background gas in a

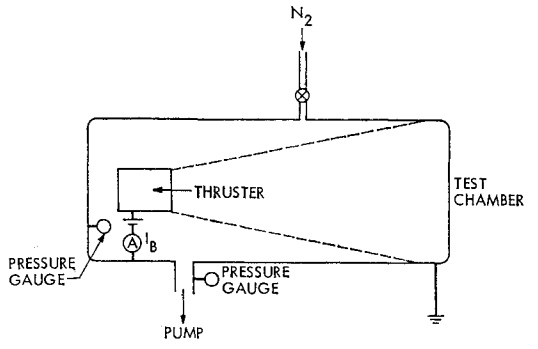

Fig. 11 Nitrogen flow test setup for measuring back ingestion.

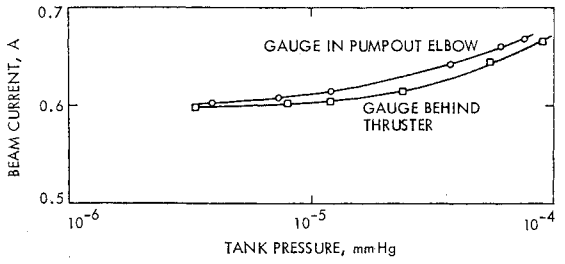

Fig. 12 Beam current dependence on background pressure.

vacuum facility is not normally pure N_2, it was felt that this was a convenient technique for examining background gas effects.

Typical results of such tests are shown in Fig. 12, where electrical meter measured beam current is plotted vs chamber pressure measured at the two locations. Note that, although the two curves differ slightly, the shapes are similar. Hence, the location of the pressure gage is probably not important if an accurate calibration exists for thruster operation in the test facility. This figure does show, however, that above the normal operating pressure of this facility ($\sim$6-9 $\times$ 10^{-6} torr) measured thruster parameters are appreciably affected by the background gas.

Further tests, at constant mercury propellant flow, have shown also that the increase in beam current is not due appreciably to back-scatter of mercury into the thruster. Particularly, mass spectrometer analysis of the thruster beam shows the mercury ion content to remain approximately constant as the background pressure is increased. In Fig. 13, a typical mass spectrum is shown at 9.7 $\times$ 10^{-6} torr chamber

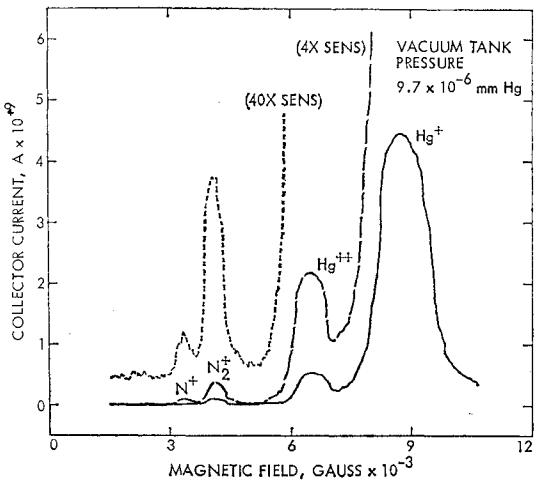

Fig. 13 Typical mass spectrum with nitrogen flow.

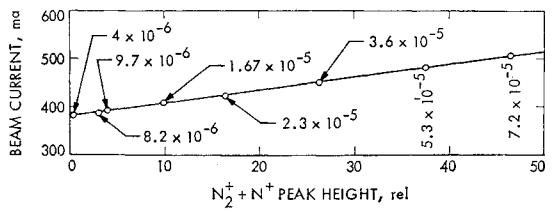

Fig. 14 Beam current dependence on total nitrogen measured in beam.

pressure. The presence of $N_2^+ + N^+$ is clearly seen, indicating that the nitrogen is directly taken into the thruster and ionized.

A summary of the mass spectrometer data is given in Fig. 14. Here, the total relative nitrogen ion content ($N_2^+ + N^+$) of the beam is shown to give a linear increase of the measured beam current. For reference, the chamber pressure corresponding to each measurement is also indicated. Note that by simply extrapolating this straight line to zero nitrogen ion content the true beam current at zero background pressure can be determined. For the normal operation-pressure of this facility, about 10 ma beam current could be the result of back ingestion. This represents about 2.6% error in the electric meter beam current measurement.

These studies have shown that the test facility must be "calibrated" to determine the relative effects of the test environment on apparent thruster performance. Any measurement of such parameters as mass utilization and beam current must take such a calibration into account.

Propellant Flow Rate

The measured flow rate to the thruster was investigated in some detail as a result of propellant utilization measurements showing greater than 100% utilization. The most significant variation in mercury flow rate measurements appeared to be the sensitivity of the flow measuring apparatus to changes in pressure. As the propellant is consumed by the thruster, the pressure is reduced in the propellant system since the pressure head is reduced. When the weight of the mercury required to restore the pressure head to its initial level was measured, it was always found to be greater than the weight calculated from the volume used during a measured time interval. These results are shown in Fig. 15. Average flow errors on the

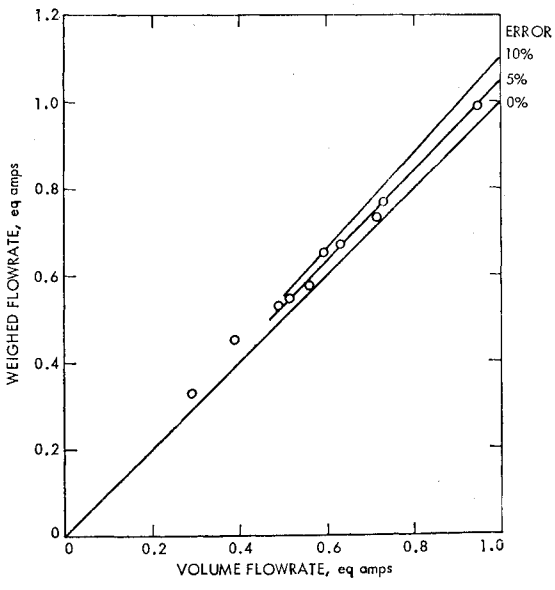

Fig. 15 Flow rate error between weighed amounts and volume calculated mercury weight.

order of 8% were found to exist. The reasons for the sensitivity to pressure are not known at this time. It is concluded, however, that the most meaningful indication of the propellant flow rate is the weight of the amount of mercury required to restore the system to a constant pressure level after the thruster has operated for a long interval at constant operating power.

Summary of Results

A typical 20-cm-diam ion thruster was examined to determine the thruster performance more accurately than could be determined from only the electrical parameter measurements that are normally used. A unique method of accurately evaluating ion beam spreading was developed and used to determine the thrust loss from this mechanism. Double ion content was determined with the use of a simple mass spectrometer. A hitherto undetected variation in double ion content across the diameter of the thruster was observed. The mass spectrograph also proved useful in determining the amount of propellant back ingested from the vacuum facility. A variation between weighed and volumetrically measured mercury flow rates was also noted.

The contribution from what are felt to be major error sources within the thruster are listed in Table 1. The parentheses indicate errors dependent on the test facility. The thrust, as determined by electrical parameters, would be too high by at least 7%. Propellant utilization could be about 14% lower than measured and the actual specific impulse would be about 15% lower than indicated. The propellant utilization numbers are, of course, very dependent on the vacuum facility and design of the propellant feed system. Some further correction may also be necessary from secondary error sources.

It has been shown that several significant errors may be present in the usually quoted performance numbers of a typical ion thruster. An accurate calibration of the thruster and the test facility is therefore necessary in identifying these errors so that accurate performance levels can be made available for accurate mission analysis.

Table 1 Calibration errors

	Thrust %	Propellant % flow	Specific % impulse
Ion beam spreading	−2.5	—	−2.5
Double ion content	−2.0	−3.2	−1.9
Back ingestion	(−2.6)	(−2.6)	(−2.6)
Flow rate		(−8.0)	−(8.0)
Total error	−4.5	−3.2	−4.4
	(−7.1)	(−13.8)	(−15.0)

References

[1] "Solar Electric Propulsion Asteroid Belt Mission Study," Final Report on JPL Contract 952566, Doc. SD-70-21, Jan. 1970, North American Rockwell, Downey, Calif.

[2] "Study of a Solar Electric Multi-Mission Spacecraft," Final Report on JPL Contract 952394, Doc. 09451-6001-RO-02, Jan. 1970, TRW Inc., Redondo Beach, Calif.

[3] Bartz, D. R. and Horsewood, J. L., "Characteristics, Capabilities, and Costs of Solar-Electric Spacecraft for Planetary Missions," AIAA Paper 69-1103, Anaheim, Calif., 1969.

[4] Wrobel, J. R. and Kerrisk, D. J., "Early Exploration of the Asteroids Region by Solar Powered Electrically Propelled Spacecraft," Paper XA. 4 Joint National Meeting of the American Astronautics Society (15th Annual) and the Operations Research Society (35th National), Denver, Colo., June 1969.

[5] Kerrisk, D. J., "Implications of Electric Propulsion Systems for Spacecraft Designs," presented at the ASME Space Technology and Heat Transfer Conference, Los Angeles, Calif., June 1970.

[6] Pawlik, E. V., "Performance of a 20-cm Hollow Cathode Ion Thruster," TM 33-468, Feb. 15, 1971, Jet Propulsion Lab., Pasadena, Calif.

[7] Pawlik, E. V. and Fitzgerald, D. J., "Cathode and Ion Chamber Investigations on a 20-cm Diameter Hollow Cathode Ion Thruster," AIAA Paper 71-158, New York, 1971.

[8] Pawlik, E. V. et al., "Ion Thruster Performance Calibration," AIAA Paper 72-475, Bethesda, Md., 1972.

[9] Byers, D. C., "Angular Distribution of Kaufman Ion Thruster Beams," TN D-5844, June 1970, NASA.

[10] Lathem, W. C. and Hudson, W. R., "Operational Characteristics of a Translation Screen Grid Beam Deflection System for a 5-cm Kaufman Thruster," TMX-68008, Jan. 1972, NASA.

[11] Junge, H. J., "Direkte Schubmessungen Am Ionentriebwerk ESKA 18P," *Proceedings of the DGLR Symposium Elektrische Antriebs Systeme*, DLR Mittulung 71-22, Braunschweig, June 1971.

[12] Masek, T. D., "Plasma Properties and Performance of Mercury Ion Thrusters," TR 32-1483, June 15, 1970, Jet Propulsion Lab., Pasadena, Calif.

[13] Milder, N. L., "Comparative Measurements of Singly and Doubly Ionized Mercury Produced by Electron-Bombardment Ion Engine," TN-1219, July 1962, NASA.

[14] Kemp, R. F., Sellen, J. M., and Pawlik, E. V., "Beam Neutralization Tests of a Flight Model Electron Bombardment Engine, ARS Paper 2663-62, 17th Annual Meeting and Space Flight Exposition, Los Angeles, Calif., Nov. 1962.

[15] Kieffer, L. J., "Compilation of Low Energy Electron Collision Cross Section Data," JILA Information Center Report 6, Part I, Joint Inst. for Lab. Astrophysics, Boulder, Colo., Jan. 10, 1969.

[16] Goldstein, R., "Numerical Calculation of Electron-Atom Excitation and Ionization Rates Using Gryzinski Cross Sections," TR 32-1372, March 1, 1969, Jet Propulsion Lab., Pasadena, Calif.